Shallow and deep traps in conjugated polymers of high intrachain order

W. Graupner, G. Leditzky, and G. Leising
Institut für Festkörperphysik, Technische Universität Graz, Petersgasse 16, A-8010 Graz, Austria

U. Scherf
Max-Planck-Institut für Polymerforschung, Ackermannweg 10, D-55128 Mainz, Germany
(Received 17 May 1996)

We present measurements of thermally stimulated currents and photoinduced absorption (PIA) in a planarized form of poly(para-phenylene). Due to the high intrachain order of the samples and their narrow distribution of effective conjugation lengths the density of states shows a very steep onset at the band gap energy. This is the prerequisite for detecting distinct trap levels and to determine their concentration and depth. We show that charges trapped at depths of 0.1 and 0.4 eV govern the observed charge transport and change in the absorption upon photoexcitation and in particular that the temperature dependence of the PIA intensity in the millisecond range reflects thermal effects on transport processes. [S0163-1829(96)05435-5]

I. INTRODUCTION

Recently it was shown that the wide gap semiconductor poly(para-phenylene) (PPP) can be used as the active layer in blue-light emitting devices [LED].[1,2] The electronic properties of conjugated polymers depend strongly on their structural regularity. The motivation for the synthesis of poly(para-phenylene) ladder polymers (LPPP's) with a chemical structure shown in Fig. 1 was the better overlap of the π electrons achieved by a planarization of the polymer backbone.[3] At the same time the synthesis via a polymer-analogous ring closure reaction of a substituted polymer backbone[4] results in a polymer structure with a very narrow conjugation length distribution. In conventional routes to PPP's defects like branched chains and large torsion angles of neighboring rings are known to occur. These defects act as electron and/or hole shallow or deep traps[5,6] which limit the mobility of charge carriers.[7] The synthetic route towards the PPP-type ladder polymers prevents the described defects.

These properties lead to an excellent performance of the LPPP's in LED's.[8,9] The well-defined conjugation length and high intrachain order of these polymers seems to be responsible for effects like the lack of competition between photoinduced absorption and stimulated emission[10] which makes the ladder polymers promising candidates for optoelectronic devices.[11] The defined conjugation length implies a steep onset of the density of states at the band edges, which is seen in the optical absorption.[12,13] This steep onset is the prerequisite to observe well-defined trap levels by thermal release of trapped charges since the broad distribution of conjugation lengths in other conjugated polymers leads to a spatial dependence of the energy gap or highest occupied molecular orbital, lowest unoccupied molecular orbital (HOMO LUMO) distance often obscuring the analysis of experiments.[14]

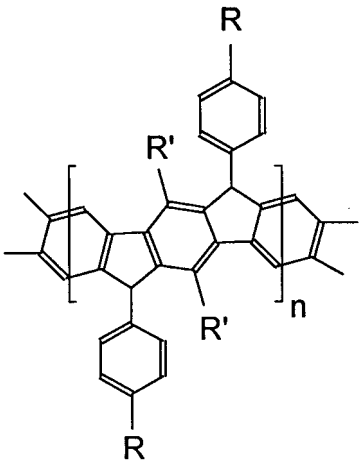

FIG. 1. Chemical structure of LPPP. $R=C_{10}H_{21}$, $R'=C_6H_{13}$, $n=20$.

Also, a very small Stokes shift is observed between absorption spectra and photoluminescence emission spectra.[15] This is the result of the suppression of geometrical relaxation of the backbone upon electronic excitation. In ordinary PPP however, the coplanar (quinoid) structure exists only in the excited state due to rotational degrees of freedom between neighboring rings.

The photoinduced spectra of the LPPP's in the near and mid infrared are known to originate from vibronic modes and electronic transitions of charged species.[16] Therefore we will compare the results of the thermally stimulated currents (TSC's) experiments, which are sensitive to mobile thermally released charges, trapped after photoexcitation, to the temperature dependence of the PIA signal, which is also due to charged states.

II. THERMALLY STIMULATED CURRENTS

For the characterization of the trap levels we applied the thermally stimulated current technique following the initial rise method,[17] which was successfully applied to other conjugated polymers.[18] The device consisted of a sapphire substrate with an interdigital gold electrode structure on top of which a 200-nm-thick polymer film was drop cast. The gold electrodes have an overall length of 87.5 cm and a gap of 20 μm. The substrate was mounted in a cryostat and cooled

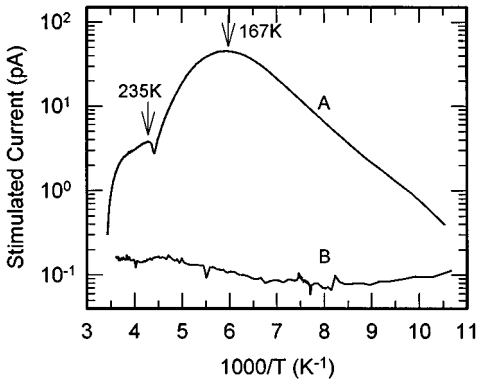

FIG. 2. Thermally stimulated current with (A) and without (B) prior illumination.

down to 90 K. After illumination of the active area of the device at 454 nm for 2 min a voltage was turned on yielding an electrical field of 4×10^4 V cm^{-1} across the electrodes. Variation of the voltage between 40 and 80 V across the gap did not result in any qualitative changes of the observed TSC's. Any increase of the duration of illumination above 2 min does not result in a greater TSC—therefore 2 min of illumination under the chosen conditions result in saturation (filling of all available traps). As the temperature T of the device was increased we observed the stimulated current depicted in Fig. 2. Trapped charge carriers are thermally released and create an electric current. As the linear heating rates were varied between 0.06 K s^{-1} and 0.25 K s^{-1} the maximum current always appeared at 167 K. This can be attributed to a monomolecular kinetics with nonretrapping traps.[17] Without prior illumination no significant current change is detectable during the heating cycle [Fig. 2(b)].

The electrical current of a coplanar interdigital gold solidus LPPP gold device is space-charge limited due to p-type charge carrier traps localized in the band gap.[12] This can be inferred from the field dependence of the dark current at room temperature. The thermally stimulated current spectrum exhibits two peaks corresponding to two distinct trap levels E_t^1 and E_t^2 which can be calculated from the rise of the current I below the peak temperature.

$$\ln I = -\frac{E_t}{k_B T} + \text{const.} \tag{1}$$

By the integration of current over time for each peak we determine the number of charge carriers which equals the number of traps N_t under the condition that all traps were occupied at the starting temperature:

$$\int_{\text{peak}} I dt = eN_t, \tag{2}$$

where e denotes the elementary charge. In Table I the results for the trap depth and the trap concentration n_t are summarized. For a typical LPPP film a density of 0.6 g cm^{-3} is observed. Via the molecular weight of the monomer unit of around 800 g mol^{-1} and the density of the polymer films the trap density per monomer unit can be calculated. The values are 0.0002 and 0.00003 traps per monomer unit, respectively.

TABLE I. Trap depth and density in LPPP; T_m temperature at peak current, E_t^{TSC} and E_t^{PIA} are the trap levels obtained from the TSC and PIA experiments respectively, N_t and n_t are the number of traps and the trap concentration, respectively.

T_m (K)	E_t^{TSC} (eV)	E_t^{PIA} (eV)	N_t	n_t (cm^{-3})
167	0.11	0.12	3.6×10^{11}	1.0×10^{17}
235	0.4	0.37	5.6×10^{10}	1.6×10^{16}

The schematic band diagram in Fig. 3 illustrates the trap distribution in the band gap. The assumption of a trap distribution mainly centered around two energetic levels is backed by the results obtained upon varying the heating rate, which gives only a corresponding change of the current intensity but no changes in the peak shape and the position of the maximum of the TSC (curve A) depicted in Fig. 2; in particular no additional features appear in the peak.

III. PHOTOINDUCED ABSORPTION

The PIA investigations were done under dynamic vacuum ($p<10^{-5}$ mbar) and at 77 K with films cast from toluene solution onto KBr substrates. For the dispersive method[19,20] the globar, the KBr-prism premonochromator and the grating monochromator of a Perkin Elmer 125 ir-spectrometer were used in the spectral range of 0.25 to 1.24 eV. The pump beam was chopped mechanically using the chopper frequency as the reference for an EG&G Princeton Applied Research lock-in amplifier 124. The probe beam was chopped at a different frequency, which was used as the reference for a second lock-in amplifier (EG&G Princeton Applied Research model 5210).

The obtained PIA spectra show an electronic transition peaking at 0.26 eV accompanied by infrared active vibrational modes which reveal the charged nature of the observed states.[16,21] The dependence of the PIA intensity on temperature is depicted in Fig. 4. To interpret the magnitude of the PIA signal we want to discuss the rate equation for the photogeneration of states. It describes the change of the number of states n with respect to time t depending on the generation rate $k\rho$ (k=const, ρ excitation density) and the decay rate ln^{μ} (l inverse lifetime, μ order of kinetics) and can be written as follows:

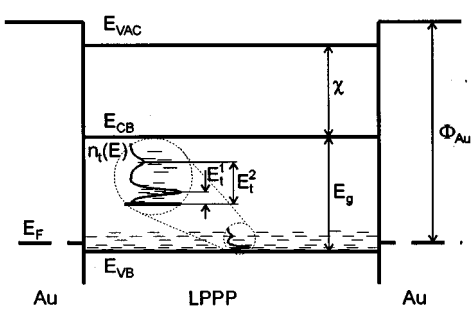

FIG. 3. Band diagram of LPPP with hole traps and gold electrodes with E_{VAC} vacuum level, E_{CB} conduction band, E_{VB} valence band, E_F Fermi level, E_g band-gap energy, E_t^1 and E_t^2 trap depths, $n_t(E)$ trap distribution, χ electron affinity, Φ_{Au} work function of the gold electrodes.

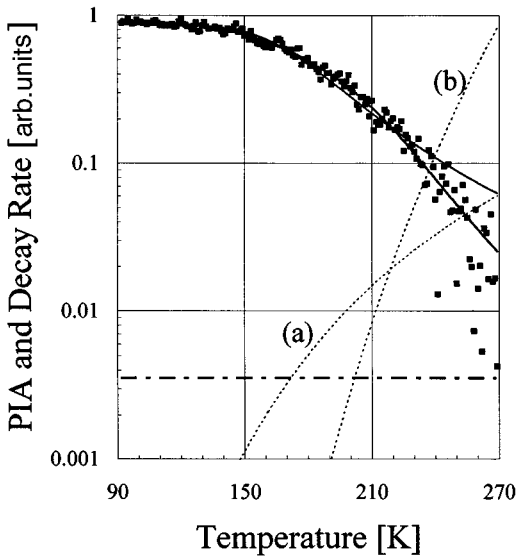

FIG. 4. PIA at 0.26 eV versus temperature (■). Full lines represent the model results obtained via Eq. (6) (lower curve for two activation energies, higher curve for one). The dotted lines represent the decay rates for the 0.12 eV (a) and 0.37 eV (b) activated process; the dash-dotted horizontal line represents the temperature independent part E.

$$\frac{dn}{dt} = k\rho - ln^{\mu}. \tag{3}$$

The number of photoexcited states in dynamic equilibrium (n_{eq}) is obtained for the decay rate equal to the creation rate [$dn/dt=0$]:

$$n_{\mathrm{eq}} = \left(\frac{k\rho}{l}\right)^{1/\mu} \propto \rho^{1/\mu}. \tag{4}$$

In a steady-state experiment, the PIA signal Y is proportional to n_{eq}. Measuring the PIA with a lock-in amplifier means to excite the sample with a periodic time-dependent pump photon flux. The latter can be approximated by a square wave that switches between a constant flux and zero photons with a frequency $f=1/\tau$. As shown in Refs. 22 and 23 the PIA signal measured with a lock-in amplifier (Y), shows the same functional dependence on ρ as n_{eq} in Eq. (4). For the *unimolecular* ($\mu=1$) and *bimolecular* ($\mu=2$) case the influence of τ depends on τ_l, the lifetime of the observed states as follows:

$$Y\begin{cases} = \text{const}, & \tau_l \ll \tau \\ \propto \tau & \tau_l \gg \tau. \end{cases}$$

Upon varying the chopper period between 6 and 94 ms we see a continuous increase of the signal with increasing chopper period ($\sim\tau^{0.65}$). Since Y is not linear in τ at 100 ms, τ_l has to be of the order of 100 ms.

Assuming l to be the only temperature-dependent factor, which represents a decay rate varying with T, changes Eq. (4) to

$$n_{\mathrm{eq}}(T) = \left(\frac{k\rho}{l(T)}\right)^{1/\mu} \propto \left(\frac{1}{l(T)}\right)^{1/\mu}. \tag{5}$$

A satisfactory description of our experimental results is obtained for a $n_{\mathrm{eq}}(T)$ of the following form:

$$n_{\mathrm{eq}}(T) = A\left(\exp\left[\frac{-W_1}{k_B T}\right] + B\,\exp\left[\frac{-W_2}{k_B T}\right] + E\right)^{-1/\mu}. \tag{6}$$

Here, k_B is Boltzmann's constant, A represents a normalization factor, W_1 and W_2 are the activation energies for a thermally enhanced decay of the photoinduced states, E is the temperature-independent part of the decay factor l, and finally B represents the relative weight of the W_2-activated process.

The exponent $1/\mu$ in Eq. (5) was found to be 0.65 for our samples.[16] With this value we tried to model the experimental curve in Fig. 4 by Eq. (6). We obtained 0.12 and 0.37 eV for the energies W_1 and W_2, respectively. The parameters B and E are 1.17×10^{6} and 3.90×10^{-4}. These numbers mean that the 0.12 eV process reaches the magnitude of the temperature-independent decay rate (E) at 170 K, while the 0.37-eV process reaches this level at 200 K and becomes the dominant decay channel above 220 K (Fig. 4). We checked the quality of the obtained parameters by setting B equal to zero (i.e., using only one activation energy). This results in an activation energy of 0.17 eV, an increase of the error sum by about 30% and a mediocre description of the observed curve at temperatures above 240 K (Fig. 4). This effect is due to neglecting the deeper trap at about 0.37 eV which dominates the recombination rate at temperatures above 220 K. A variation of the activation energies by more than 3% of the quoted values resulted in increasing the error sum significantly.

IV. DISCUSSION

First, we want to address the question of how sample quality influences the observed results. Synthesis and sample treatment influence the electronic properties of these materials in a defined way.[13] We have already shown [16,21] that the shape and intensity of photoinduced absorption spectra in different representatives of the LPPP's may vary, indicating at least different trap densities but also different electronic properties of these traps, depending on the synthesis and subsequent treatment of the polymers. However the electronic properties for this class of polymers can be understood in terms of effective conjugation length [8,13,15,24] charge transfer by photoexcitation or redox reactions[21,16] and photooxidation upon intense visible irradiation under the influence of oxygen.[13] Therefore by optical spectroscopy (absorption, photoluminescence, photoinduced absorption) we can very well assess the quality of a sample.

For the LPPP's studied in this work, we have shown by comparing optical and transport properties, that both thermally induced transport and photoinduced absorption are governed by the same traps. Concerning the nature of electronic traps in this class of ladder polymers we want to recall the experimental facts: When comparing the LPPP results to experiments on poly(para-phenylene vinylene) (PPV) (Ref. 25) we have to stress that the appearance of the maximum current at 167 K for heating rates between 0.06 K s^{-1} and 0.25 K s^{-1} can be attributed to a monomolecular kinetics with nonretrapping traps.[17] In PPV the density of trap states is evaluated on the base of a multiple trapping model [25]

leading to a trap density which is comparable to the density of monomer units and very low mobilities of 10^{-8} cm^2/V s. These values for PPV have to be compared to trap densities of 0.0002 and 0.00003 traps per monomer unit in the LPPP. In accordance with the low trap densities one also obtains high mobility values of 0.1 cm^2/V s for the LPPP's.[26]

The photoinduced absorption and the electrical characteristics of the conjugated LPPP show that the optoelectrical properties are strongly dependent on charge carrier traps in the band gap. From aromatic molecular crystals it is known that impurities and structural imperfections form localized states.[27] LPPP forms homogeneous and dense films with a mean interchain distance of about 20 Å and negligible long-range order. We propose that the 0.1-eV trap level is a result of local variations of the electronic band structure due to the influence of neighboring molecules (aggregates or small crystallites). The 0.4-eV level occurs in a much lower concentration and results from chemical defects in the polymer backbone or impurities which break the conjugation of the polymer.

An alternative interpretation for the activated behavior of the photocurrent and the PIA decrease with temperature was put forward by Townsend *et al.*[28] They assigned their experimental results obtained on Durham *trans*polyacetylene to a thermally activated *interchain-hopping* mechanism for bipolaronlike charged soliton pairs.

In electroluminescence devices (LED's) ionized traps form space charges, which govern the charge carrier injection from metal electrodes into the active material.[7] The same states that trap charge carriers may also act as recombination center for the nonradiative decay of excitons. Therefore the luminescence efficiency as well as charge carrier transport in LED's are influenced by traps. Both factors determine the quantum efficiency of LED's.

The excellent agreement between TSC and PIA results has two implications. First, since the TSC method probes the product of mobility and carrier density while the PIA probes only the carrier density there seems to be no dominant influence of the temperature dependence of the carrier mobility. This was also found in other conjugated polymers like *trans*polyacetylene.[5,29] Second, photoconductivity (observed via the thermal release of photoexcited and trapped carriers) and photoinduced absorption probe the same charged entity.[29–31]

In conclusion, we have determined the concentration of traps located at 0.1 and 0.4 eV in a conjugated ladder polymer. The deeper traps occur at a concentration of 1.6×10^{16} cm^{-3}, about a factor of 6 lower than the shallow traps. Compared to other conjugated polymers the observed trap densities are lower by orders of magnitude. These traps govern both charge transport and the optical absorption and are therefore important in the operation of optoelectronic devices.

ACKNOWLEDGMENTS

The financial support by the Austrian Fonds zur Förderung der wissenschaftlichen Forschung, projects No. P 9091 CHE and P 9300 TEC, which is a part of the BRITE/EURAM project HICOPOL, is gratefully acknowledged.

[1] G. Grem, G. Leditzky, B. Ullrich, and G. Leising, Adv. Mat. **4**, 36 (1992).
[2] G. Grem, G. Leditzky, B. Ullrich, and G. Leising, Synth. Met. **51**, 383 (1992).
[3] J. L. Bredas, B. Thermanns, J. G. Fripiat, and J. M. Andre, Phys. Rev. B **29**, 6761 (1984).
[4] U. Scherf and K. Müllen, Makromol. Chem. **12**, 489 (1991).
[5] D. Moses and A. J. Heeger, in *Relaxation in Polymers*, edited by T. Kobayashi (World Scientific, Singapore 1993).
[6] B. R. Hsieh, H. Antoniadis, M. A. Abkowitz, and M. Stolka, Polym. Preprints **33**, 414 (1992), and references therein.
[7] H. Antoniadis, M. A. Abkowitz, and B. R. Hsieh, Appl. Phys. Lett. **65**, 2030 (1994).
[8] G. Grem, C. Paar, J. Stampfl, G. Leising, J. Huber, and U. Scherf, Chem. Mater. **7**, 2 (1995).
[9] S. Tasch, A. Niko, G. Leising, and U. Scherf, Appl. Phys. Lett. **68**, 1090 (1996).
[10] W. Graupner, G. Leising, G. Lanzani, M. Nisoli, S. De Silvestri, and U. Scherf, Phys. Rev. Lett. **76**, 847 (1996).
[11] T. Pauck, R. Hennig, M. Perner, U. Lemmer, U. Siegner, R. F. Mahrt, U. Scherf, K. Müllen, H. Bässler, and E. O. Göbel, Chem. Phys. Lett. **244**, 171 (1995).
[12] G. Leditzky and G. Leising, J. Phys. D **27**, 2185 (1994).
[13] W. Graupner, S. Eder, M. Mauri, G. Leising, and U. Scherf, Synth. Met. **69**, 419 (1995).
[14] E. M. Conwell, L. J. Rothberg, and H. A. Mizes, Phys. Rev. Lett. **73**, 3179 (1994).
[15] J. Stampfl, W. Graupner, G. Leising, and U. Scherf, J. Lumin. **63**, 117 (1995).
[16] W. Graupner, M. Mauri, J. Stampfl, G. Leising, U. Scherf, and K. Müllen, Solid State Commun. **91**, 7 (1994).
[17] G. A. Dussel and R. H. Bube, Phys. Rev. **155**, 764 (1967).
[18] M. Onoda, D. H. Park, and K. Yoshino, J. Phys. C **1**, 113 (1989).
[19] Z. Vardeny, J. Orenstein, and G. L. Baker, J. Phys. (France) Coll. **44**, 325 (1983).
[20] P. O'Connor and J. Tauc, Phys. Rev. B **25**, 2748 (1982).
[21] W. Graupner, M. Mauri, J. Stampfl, O. Unterweger, G. Leising, U. Scherf, and K. Müllen, Mol. Cryst. Liq. Cryst. **256**, 431 (1994).
[22] J. M. Leng, R. P. McCall, K. R. Cromack, Y. Sun, K. Manohar, A. G. MacDiarmid, and A. J. Epstein, Phys. Rev. B **48**, 15 719 (1993).
[23] C. Botta, S. Luzzati, R. Tubino, and A. Borghesi, Phys. Rev. B **46**, 13 008 (1992).
[24] J. Grimme, M. Kreyenschmidt, F. Uckert, K. Müllen, and U. Scherf, Adv. Mat. **7**, 292 (1995).
[25] H. Meyer, D. Haarer, H. Naarmann, and H. H. Hörhold, Phys. Rev. B **52**, 2587 (1995).
[26] G. Leditzky, Ph.D. Thesis, Graz University of Technology, Graz Austria, 1994.
[27] E. A. Silinsh, Phys. Status Solidi A **3**, 817 (1970).
[28] P. D. Townsend and R. H. Friend, Phys. Rev. B **40**, 3112 (1989).
[29] M. Sinclair, D. Moses, and A. J. Heeger, Solid State Commun. **59**, 343 (1986).
[30] D. Moses, M. Sinclair, and A. J. Heeger, Phys. Rev. Lett. **58**, 2710 (1987).
[31] L. Rothberg, T. M. Jedju, P. D. Townsend, S. Etemad, and G. L. Baker, Phys. Rev. Lett. **65**, 100 (1990).